Effects of profile errors on lubrication performance of helical gears

A. Clarke*[a], H.U. Jamali[b], K. J. Sharif[a], H.P. Evans[a], R. Frazer[c], B. Shaw[c]

a School of Engineering, Cardiff University, Cardiff, United Kingdom.

b College of Engineering, Karbala University, Karbala, Iraq.

c Design Unit, Newcastle University, Newcastle, United Kingdom.

* corresponding author – clarkea7@cardiff.ac.uk

1. ABSTRACT

Analysis of the elastohydrodynamic lubrication (EHL) of gears generally assumes that the tooth flanks are smooth surfaces. There is considerable interest in establishing the extent to which smooth surface analyses are distorted by the presence of surface roughness. The current paper concerns a different scale of deviation from the specified surface profile, namely involute profile error. The paper quantifies the deviation from the smooth surface behaviour using standard profile error measurements, and also considers how the means by which profile error is measured influences the outcome/conclusions. Transient EHL analyses of the meshing cycle of helical gears taking profile error data from a gear measuring machine are compared with analyses using equivalent measurements determined by the waviness from surface profilometer measurements.

Keywords: gears; lubrication; profile errors; EHL

2. INTRODUCTION

Profile error in gear manufacture is known to be important in terms of the smooth running and noise characteristics of gear drives. These effects influence the dynamic behaviour of a gear pair and have generally been considered in that context. For example, Kahraman and Singh [1] as part of their investigation into non-linear dynamics of spur gears, whilst Fernandez et al. [2] considered both profile errors and profile modification in a further spur gear dynamic model. Ottewil et al. [3] considered relatively minor profile errors to be a contributory factor to gear noise and rattle problems, and found good agreement between the predictions of their model and experimental measurements. Other workers [4] have used similar dynamics models to quantify the effects of profile errors on

1

vibration characteristics of gear trains. Other workers have considered the effects of profile error on contact stress and root bending stress in addition to dynamic effects [5], and the effects of wear-induced profile deviations [6] but these stress calculations are all based on dry contact analyses. In contrast, almost no attention has been paid to profile error in terms of its influence on the lubrication characteristics of the gear pair. It is measured as a means of assessing the accuracy of the manufactured gear and this is done with dedicated gear measuring machines or on coordinate measuring systems.

Elastohydrodynamic lubrication of gears has been studied widely, and indeed this application is one of the main engineering applications of EHL theory. Gear design methods use EHL theory in the form of steady state line contact analysis of the well-known Dowson and Higginson formula [7]. The action of a gear pair is only approximately steady state as the load applied, the radius of relative curvature and the surface kinematics vary over the meshing cycle. In spur gears the load variation includes rapid change at the points in the meshing cycle where the number of tooth pairs in mesh changes. Models of the gear meshing cycle have evolved from the earliest and simplest type which consider a sequence of steady state models, such as the work of Simon [8], Zhu *et al.* [9] on helical gears, to transient analyses such as Li *et al.* [7] where the time varying effects are included in the analysis. Such transient EHL analyses have taken into account dynamic variation of meshing conditions and tooth load over the meshing cycle [10], impact loads during gear meshing [11] and thermal effects [12].

There is a clear awareness that smooth surface film thicknesses are only part of the story as the presence of surface roughness can be a highly influential factor in determining the successful operation of a gear pair. Many authors have studied the effects of surface roughness in the EHL contact between gear teeth incorporating different degrees of reality/complication. Including surface roughness makes the problem strongly time dependent and highly demanding as it has to be resolved at the scale of the surface roughness features. Most of these studies have been of the line contact form because the lay of the surface finish lends itself well to that simplification. This is particularly so for spur gears because the contact lines are parallel to the gear axes but less so for helical gears where the contact lines are inclined to the gear axes. Approaches have included transient simulations using measured roughness profiles at a number of discrete positions through the meshing cycle [13], models which treat the roughness statistically [14], and in a meshing cycle model where the mixed lubrication conditions are approximated by interpolating between a smooth EHL result and a dry contact rough surface result [15].

Whilst many have approximated the contact of helical gears as a series of narrow width spur gears [16], full 3D EHL models of the meshing cycle in helical gears are less common although the results

2

of several such investigations have been reported by researchers [17, 18, 19]. The analysis reported in [19] was concerned with the transient effects of micro-profile modifications such as tip relief and axial crowning. In the current study the analysis has been developed to include involute profile error measurements as part of the definition of the tooth flank geometry so that the effect of the measured local deviations from the involute shape can be quantified in terms of the lubricant pressure and film thickness and their deviations from the equivalent smooth surface analysis. Results are presented for analysis of the effects of profile deviations measured from helical gear pairs used in a separate testing programme.

3. NOTATION

E'	Reduced elastic modulus of contact.	Pa
f	Pressure influence coefficients in equation (2)	m^{-1}
F	Gear face width	m
h	Lubricant film thickness.	m
h	Form height measurement in section 4.	m
h_{fit}	Involute curve fit to form height.	m
h_{diff}	Form height minus involute fit height.	m
h_u	Undeformed gap between surfaces	m
i, j, k, l	Grid point indices	
p	Lubricant pressure.	Pa
s	Distance from pitch line in plane of contact.	m
SAP	Start of active profile position.	
STR	Start of tip relief position.	
S_x, S_y	Non-Newtonian flow parameters	
T	Time.	s
$\bar{u}$	Mean velocity of surfaces relative to contact line	$m.s^{-1}$
x	Coordinate in tangent plane in direction of surface motion.	m
y	Coordinate in direction of contact line	M
z	Coordinate in direction of common normal to contacting surfaces.	
z'	Coordinate in plane of contact transverse to gear axis.	
β_b	Base helix angle	rad
Δ	Maximum tip relief.	m
η	Lubricant viscosity	Pa.s
θ	Angle between axial roughness features and contact line in tangent plane.	
ψ	Working pressure angle.	
ρ	Lubricant density	$kg.m^{-3}$
σ_x, σ_y	Flow factors in equation (1).	m.s

4. EHL MODELLING

The EHL model is set up in the tangent plane Oxy of the contact between the gear teeth as illustrated in Figure 1. This shows the contact line EE' which coincides with axis Oy. Oz is the direction of the common normal to the surfaces at the contact line. The motion of the surfaces relative to the contact line takes place in the Ox direction and is responsible for entrainment of lubricant into the concentrated contact occurring nominally on the contact line. Axis set O$xy'z'$ has Oy' parallel to the gear axis so that Oxz' is the transverse plane in which the gear flanks have an involute profile.
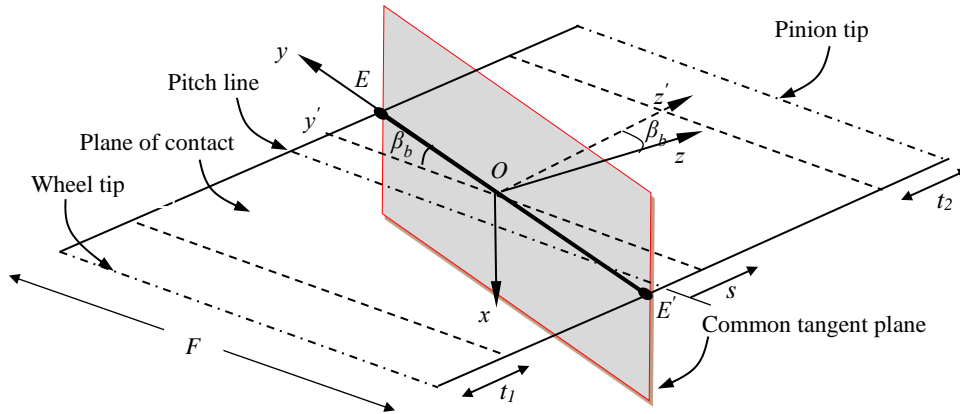

Figure 1 Schematic of plane of contact and general contact line EE'. Oxy is the common tangent plane and dimensions t_1 and t_2 indicate tip relief zones.

The equations that define the EHL problem are the Reynolds equation for the lubricant separating the surfaces, equation (1), and the elastic deflection equation, equation (2), which quantifies the change of shape of the surfaces due to the pressure developed in the fluid.

$$\frac{\partial}{\partial x}\left(\sigma_x \frac{\partial p}{\partial x}\right) + \frac{\partial}{\partial y}\left(\sigma_y \frac{\partial p}{\partial y}\right) - \frac{\partial(\rho \bar{u} h)}{\partial x} - \frac{\partial(\rho h)}{\partial t} = 0 \tag{1}$$

$$\frac{\partial^2 h(x_i, y_i)}{\partial x^2} + \frac{\partial^2 h(x_i, y_i)}{\partial y^2} = \nabla^2 h_u(x_i, y_i) + \frac{2}{\pi E'} \sum_{all\,k,all\,l} f_{k-i,l-j}\ p_{k,l} \tag{2}$$

These equations link the pressure, p, and the film thickness, h, and must be solved simultaneously. In equation (1) the terms σ_x and σ_y are

$$\sigma_x = \frac{\rho h^3}{12\eta} S_x \quad ; \quad \sigma_y = \frac{\rho h^3}{12\eta} S_y \tag{3}$$

The lubricant density, ρ, and viscosity, η, are functions of pressure, and the non-Newtonian parameters S_x and S_y depend on the local values of h, η, $\partial p/\partial x$, $\partial p/\partial y$ and the sliding speed u_s

according to the non-Newtonian rheological model adopted. The entrainment velocity $\bar{u}$ is the mean velocity of the tooth surfaces in the x direction.

Equation (2) is written in the form of a second order partial differential equation as described in [20] and involves the undeformed gap between the surfaces, h_u, and the Laplacian of the elastic deflection. It is presented here in the form of the convolution summation for a uniform grid of mesh points in the tangent plane with mesh indices i k and j l.

The undeformed gap h_u is calculated from the helical involute profile shape of each surface and the axial correction supplied to the contact which takes the form of an axial crown together with axial chamfers at the face edges. This information is calculated in the transverse plane for each of the mesh points as is the surface velocity of each tooth.

The equations are solved for the contact between one pair of gear teeth from an initial contact near the root of the pinion to a final contact near the root of the wheel. The time between these two contact positions is divided into 575 equal timesteps as described in [19], including transient variation of tooth geometry, surface velocities and load. The method of solution corresponds to that described in [19 & 21].

5. PROFILE ERROR MEASUREMENT

Standard profile error measurements for the test gears being modelled were taken with a Klingelnberg P65 gear checker (P65). This uses coordinate measurements based on contact of the gear flank with a 2 mm diameter spherical probe to provide a profile of 480 points between two specified radial positions that are equally spaced in roll angle. Figure 2 shows a plot of the standard profiles taken for a 23 tooth pinion after manufacture and prior to running.
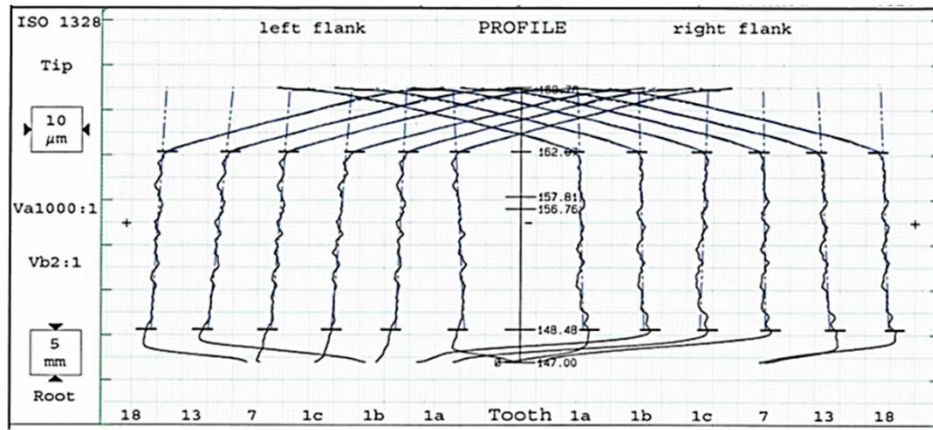
Figure 2. Example Klingelnberg P65 profile error measurements for a 23 tooth pinion

The instrument calculates the deviation from the specified involute so that a vertical line in these plots corresponds to the perfect involute curve and each profile has a straight line fitted to the measurements in the portion expected to have the involute shape, between diameters of 148.48 mm and 162.07 mm in this example. The tip relief profile is clearly visible at larger diameters and a second straight line is fitted to this portion. The gear tip is not clearly visible as the measurements chart its interaction with the 2 mm diameter sphere.

Four teeth, numbered 1, 7, 13 and 18, are at nominal 90° intervals and are measured on the axial mid plane of the gear. Additional measurements (1a and 1c) are taken of tooth 1 near to the face boundaries. There is clear similarity between the central profiles on each flank as far as inspection of the plots is concerned, and other measurements of 40 such error profiles spaced equally over the gear face width confirm that error features are a function of the roll angle with little axial variation. To introduce the error measurements to the EHL analysis the roll angle of each mesh position in the tangent plane is calculated and the corresponding measured error value for each tooth is obtained from the error profiles by cubic spline interpolation and added to the undeformed film thickness, h_u.

To take stylus profilometer profiles of the gear teeth the as-manufactured helical gears were mounted in a purpose made jig that inclines the gear axis to the vertical by the tooth base helix angle, β_b, as shown in Figure 3. The tooth surface to be measured was then nominally horizontal and rotating the gear to an optimal position enabled root to tip profile measurements to be taken within the 1 mm range of the profilometer gauge. Profiles were taken that included the gear tip as a clearly identified reference point. This was facilitated by use of an accessory that can be adjusted to provide a stop support for the stylus if it loses contact with the surface, which would otherwise cause the measurement to be automatically abandoned. The out of contact measurement is then constant.
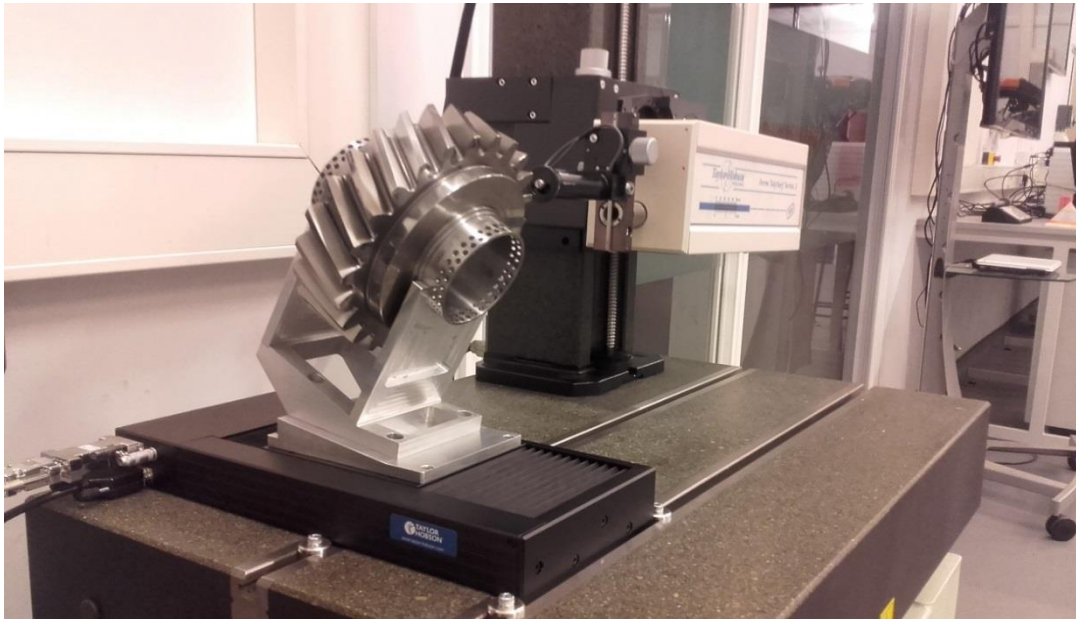
Figure 3. Photograph of gear mounted in measuring jig on profilometer y-stage.

A typical root to tip profile is illustrated in Figure 4 which consists of approximately 40,000 measured heights giving the form of the tooth and its roughness measurement. Two points of interest are identified here, T is the tip of the tooth and C is the highest point of the form. The profile heights are thus measured perpendicularly to the profile tangent at C. Due to the inclination of the gear the measurements are taken in the normal direction to the tooth flank and a $\cos\beta_b$ scaling gives the heights in the transverse plane where the form is a nominal involute.

The coordinates of C are obtained by fitting a least squares parabola to the raw data over a 2 mm length centred on the observed position of C and locating the maximum height position of this parabola. The coordinates of T are obtained by fitting two straight lines to the data on either side of T and locating their intersection. This process allows the distance TC to be obtained from the measured profile. The material removed in producing the tip relief is a specified value Δ at the tip (50 μm) and this is verified from the profile error measurements shown in Figure 2. This is taken to be removed perpendicular to the involute curve. The problem is thus to locate the point, R, on the involute curve whose tangent to the base circle, RR′, intersects the gear tip circle at T such that distance RT is equal to Δ. The radius of R from the gear axis can be calculated by repeated division. This determines the position of point T, and since its distance from point C is known, the radius of point C from the gear axis can then also be obtained by repeated division. The tip relief is specified in the gear manufacturing drawings and confirmed by the P65 profile error measurements.
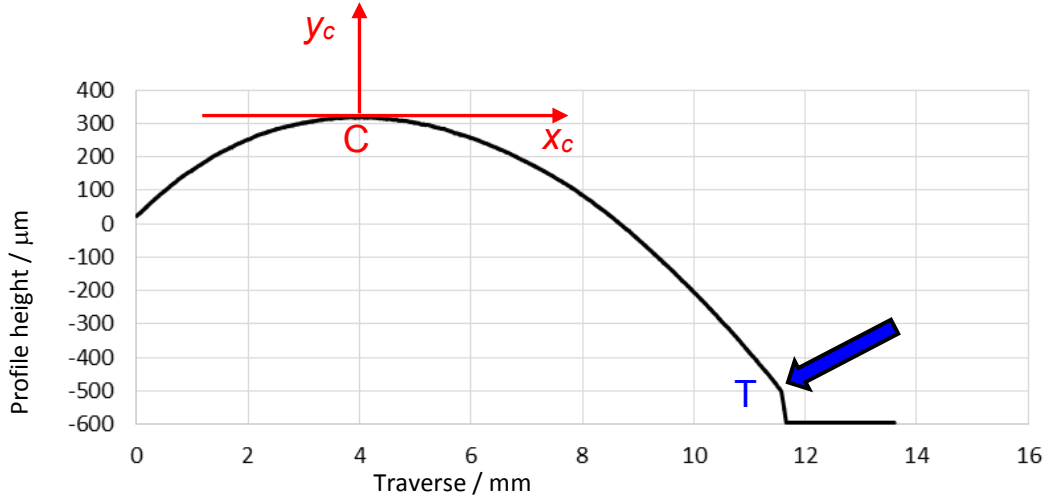
7

Figure 4. Root to tip gear profile measurement taken from test gear.

The analytic fit to the involute is used to remove the form to so that the profile gives the deviation from the involute. Figure 5 shows the measured profile in terms of roll angle which can be obtained in terms of the profile traverse coordinate from the involute geometry and the position of point C on that involute. The positions of the start of active profile (*SAP*) and tip relief (*STR*) are defined in terms of roll angle in the gear geometry specification and it is clear that the specified *STR* position corresponds to the location where the tip relief becomes apparent in the involute form-removed profile, h_{diff}.
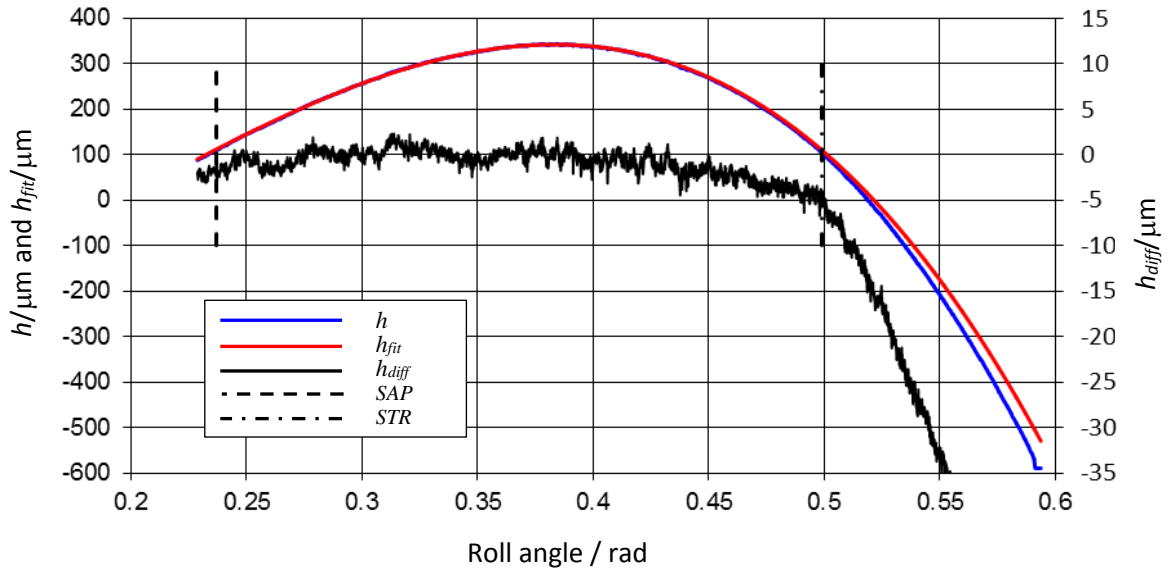

Figure 5. Profile measurement, h, involute fit, h_{fit}, and profile with fit removed, h_{diff}.
Also shown are start positions of active profile, *SAP*, and tip relief, *STR*.

Profile h_{diff} is then processed using the profilometer software. Firstly, any remaining form in the involute section is removed with a 4th order polynomial fitted between the *SAP* and *STR* positions.

This is applied to the whole profile so that the true involute section (between the *SAP* and *STR*) has a mean profile value of zero. The profile is then filtered using an ISO standard Gaussian profile to provide waviness and roughness profiles using various cut-off lengths. The waviness profiles are then further processed to provide profilometer involute profile error curves in the format of the P65 profiles. These steps are (i) to add a slope to the involute section so that it matches the slope of the P65 measurement, (ii) to add an adjustable power law to the tip relief section to counteract its new shape following the final form removal and achieve the measured tip relief at the tip, and (iii) to interpolate the data from the equally spaced x_c values in the profile measurement to the required equally spaced roll angle format of the profile error files.
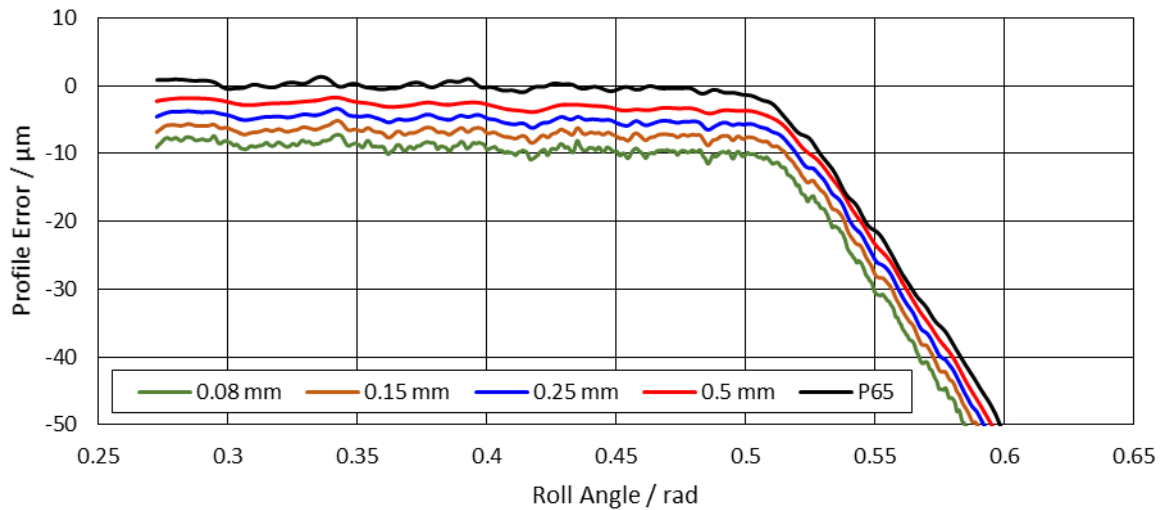

Figure 6. Profilometer involute error profiles for different filter cut off values compared with P65 error profile measured at the same position on the gear flank.

Figure 6 gives an example comparison of the profilometer based error profiles for different cut-off lengths and also with the P65 error profile obtained at the same nominal position on the tooth flank. The profiles are offset from each other for clarity and to aid comparison.

6. RESULTS

Isothermal analyses were carried out for the test gears whose dimensions are specified in Table 1, with a lubricant whose properties are specified in Table 2. The gears are manufactured from case carburised and tempered 18CrNiMo7-6 gear steel with a surface hardness of between 700 and 750 Hv, and each has a tip relief profile starting at the diameter given in table 1 that is linear with roll angle with a maximum material removal of 50 μm at the tip. The wheel teeth have a symmetric lead modification resulting in a 15 μm crown height.

Table 1. Test gear dimensions

Normal module/mm	6
Pinion tooth number	23
Wheel tooth number	24
Reference pressure angle / deg	20
Base Helix Angle / deg	26.27
Pinion tip diameter/mm	168.8
Pinion base diameter/mm	144.6
Pinion tip relief diameter/mm	162.1
Wheel tip diameter/mm	175.2
Wheel base diameter/mm	150.9
Wheel tip relief diameter/mm	168.6
Centre distance/mm	160
Face width / mm	44

Table 2. Lubricant properties

Temperature / deg C	80	90	100
Absolute viscosity / Pas	0.00708	0.00585	0.00474
Pressure viscosity coefficient / GPa	12.3	11.7	11.2

The test gears are used in micropitting, fatigue testing, and as such are lubricated with an ISO VG 100 oil in order to promote micropitting. They are subject to a load corresponding to a maximum Hertzian pressure of 1.6 GPa. Transient effects are active near the transverse limits of the EHL contact particularly when the contact line length is effectively controlled by the tip relief micro-geometry in the early and latter parts of the contact between the tooth pair. These features have been discussed in [19] and [21] and are not the focus of the current paper. For most of the EHL contact the smooth surface results are essentially a family of steady state EHL line contacts. The results presented here are aimed at identifying the effect of profile errors on the functionality of the gear contacts insomuch as in their ability to generate a lubricant film capable of separating the surfaces. To this end the comparisons are made at timestep 300 of the full transient analysis where the contact is close to the pitch point on the gear mid-plane and the adverse effects of tip relief in generating stress concentrations is relatively mild.

Figure 7 shows the pressure distribution and film thickness at timestep 300 for lubricant conditions corresponding to a temperature of 80°C where the contact line crosses the pitch line at y = -2 mm. Lubricant entrainment is in the positive x-direction and the film thickness shows two thin film lobes near the transverse limits of the contact and the characteristic exit constriction which is at around x=0.5 mm in the central part of the contact and follows the 0.4 GPa pressure contour around the exit of the contact to form a distinct exit edge constriction. The minimum film thickness is 0.24 µm. Peak pressure values of around 1.98 GPa occur in the side lobes of thin film thickness. These are associated with changes of undeformed film thickness slope in the y direction due to tip relief and the face edge chamfers. The STR positions are shown by the broken lines, and the chamfer becomes active at y = ±22 mm. The inclination of the STR lines to the y axis is due to the tip relief being imposed at the same roll angle for each position along the contact line of the helical gear as discussed below. The wheel STR line is aligned with the edge constriction whereas the pinion STR line is inboard of the side constriction. This asymmetry is due to the orientation of the STR line and the lubricant entrainment which takes place in the x direction.
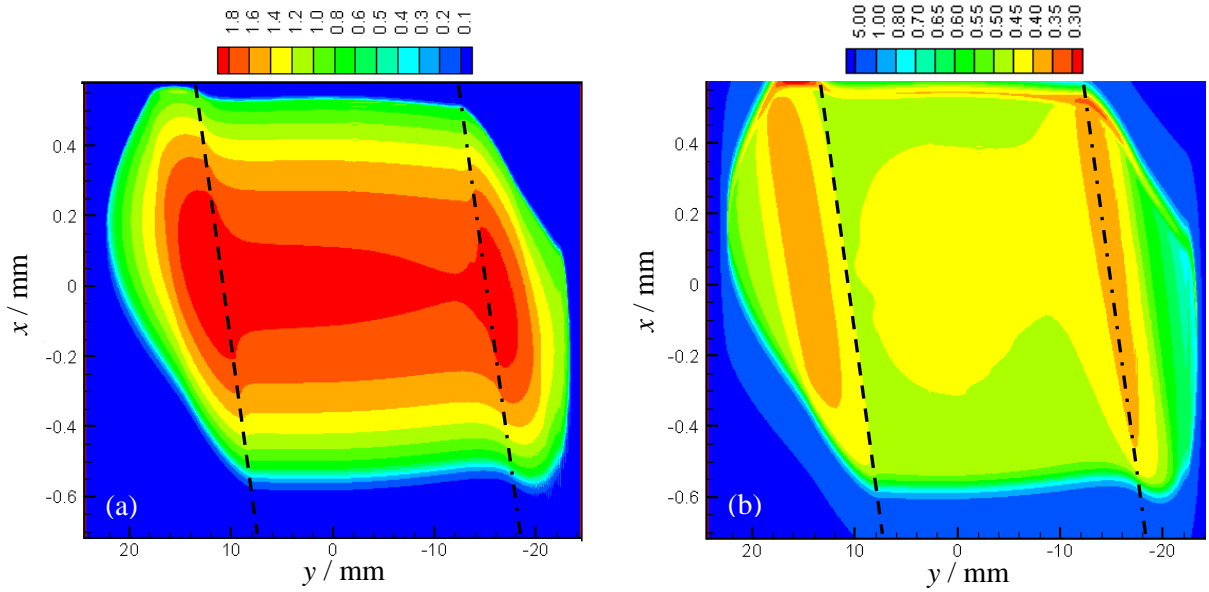

Figure 7. Contours of (a) p/GPa and (b) h/µm for the smooth surface EHL analysis at 80 ° C. Broken and chained lines indicate position of the pinion and wheel STR boundaries, respectively.

When the measured profile error is introduced into both the tooth surfaces there is a significant effect on the pressure and film thickness distributions. Figure 8 shows the result corresponding to figure 7 when the P65 profile errors are included in the calculation. (Note that the pressure and film thickness contour colours shown in Figure 8 are different to those for Figure 7 to aid comparison with the following figures).
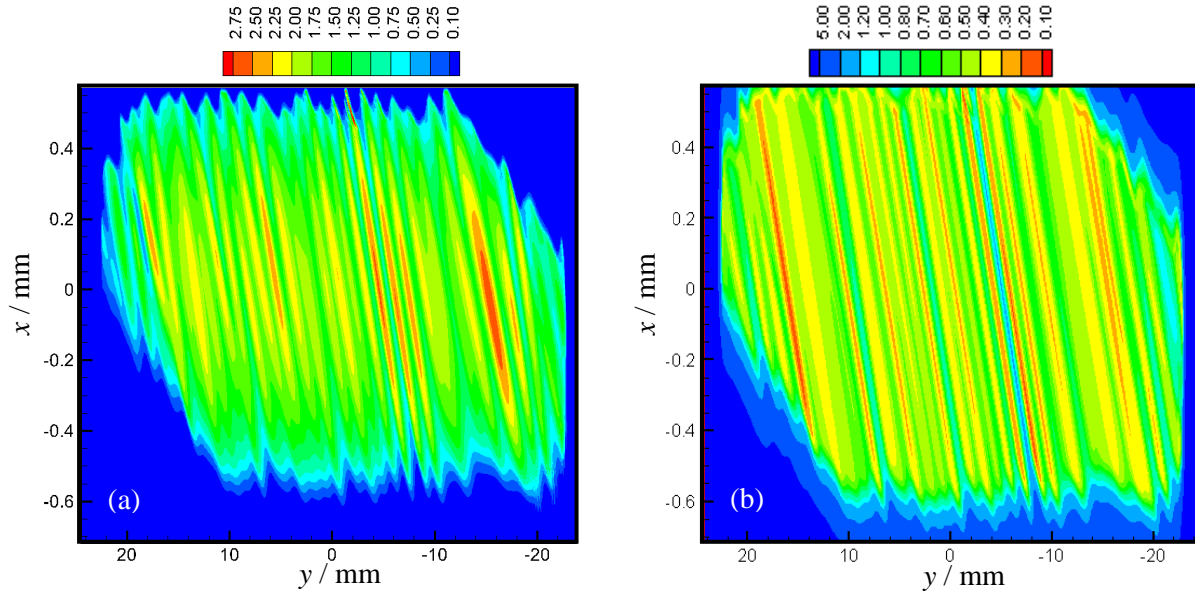
Figure 8. (a) Contours of (a) *p*/GPa and (b) *h*/μm for the EHL analysis at 80 °C
when the P65 profile errors are included.

The contour plots are presented in a near square format for clarity but it is important to realise that the scales in the *x* and *y* directions are in the ratio of about 38:1. The plots show that the effect of the profile errors is to cause significant variations in the pressure and film thickness over the whole of the contact area. For example, the peak pressure in Figure 8 is around 3.2 GPa, which is a significant increase on the corresponding maximum pressure shown in Figure 7 for the smooth surface case. Minimum film thickness is also reduced substantially to 0.09 µm, when the profile errors are taken into account.

There are a number of inclined ridges and grooves apparent in the film thickness contours. Taking the difference in the *x* and *y* direction scales into account these can be seen to be inclined at about 10° to the contact line (the *y* axis). The motion of the surfaces is in the *x* direction so that the inlet to the EHL contact is at the bottom of the figure (x = -0.5 mm) and the outlet is at the top. The ridges and grooves thus pass from the inlet to the exit of the EHL contact with corresponding high and low pressure regions that have the same inclination. The surface features measured in the profile error curves occur at the same roll angle positions across the facewidth of the tooth flank. The effect that such deviations from smoothness have on the EHL contact occur in accordance with their projection onto the contact tangent plane. For spur gears, deviation features that occur at the same roll angle across the facewidth project onto a line in the contact plane that is parallel to the contact line. However, for helical gears they project onto nearly straight curves in the tangent plane whose inclination to the contact line, θ, varies with flank position [19, 21]. At the pitch line position angle θ is given by

$$\theta = \tan^{-1}\{\sin \beta_b \tan \psi\},$$

12

where β_b is the base helix angle and ψ is the working pressure angle. The pitch line value of θ is 10.4°
for the gears considered and varies between 4.9° and 16° over the flanks as illustrated in Figure 9. In
moving away from the pitch line position the angle for one surface reduces whilst that for the other
surface increases. This feature is shown clearly in the pattern of the highest values of pressure in
Figure 8 where the contact line is the line $x = 0$. When considered closely it is apparent that there are
two families of inclined high pressure zones present. The feature crossing the contact line at $y = -4$
mm makes an angle of 10.5° with the y axis when the x and y scales are taken into account, and is
close to the pitch line. The two features that cross the contact line at y=13.3 mm and 12.8 mm make
angles of 8.8° and 13.5°, respectively and correspond to one profile error feature on the pinion surface
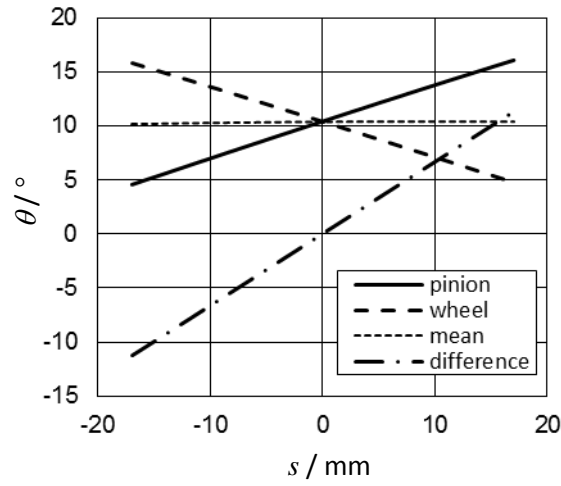and one on the wheel surface.

Figure 9. Variation of angle θ with plane of action co-ordinate, s, for the pinion and wheel flank.
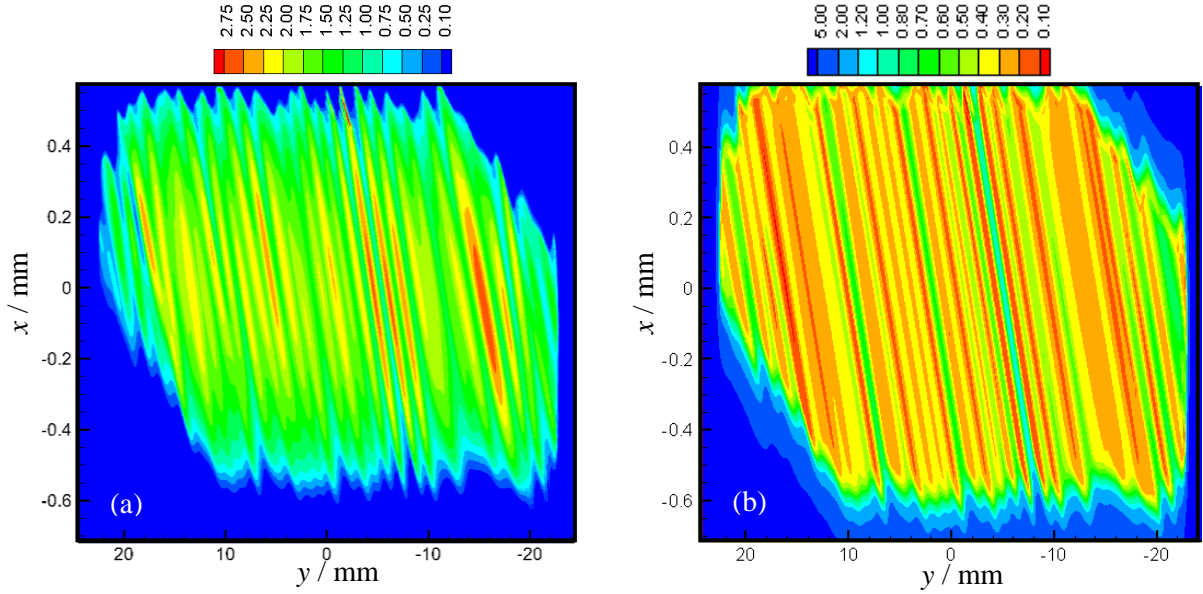Also shown are the mean value and the difference between the values.

Figure 10. (a) Contours of (a) *p*/GPa and (b) *h*/μm for the EHL analysis at 100 °C
when the P65 profile errors are included.

Figure 10 presents the pressure and film thickness distributions at timestep 300 for a higher temperature of 100 °C. This shows a similar pattern of disturbance to the film and pressure generation. The main difference in comparison with the 80 °C case is that the film thickness is reduced throughout the contact because of the change in viscosity and pressure viscosity coefficient due to the increase in temperature. There is very little difference in the pressure distribution viewed in this contour form but there are small pressure increases as the temperature is increased.

Figures 11, 12 and 13 show the results obtained at timestep 300 when the profile error information is taken from the profilometer waviness curves with filter cut-off lengths of 0.5 mm, 0.25 mm and 0.15 mm. These show that the deviations to the pressure and film thickness are determined by, and are sensitive to, the cut off length of the filter used.

For the cut off length of 0.5 mm shown in Figure 11 the perturbations to the film thickness are much lower than those shown in Figure 8. The film thickness over the smooth surface plateau area varies between 0.25 and 0.6 μm for this cut off and the corresponding pressure variations are of the order ± 0.25 GPa.

The result for a cut off of 0.25 mm shown in Figure 12 is similar to that for the P65 error profile. The film thickness in the plateau area varies between 0.18 and 0.8 μm with the pressure varying between 1 and 2.5 GPa. At the smaller cut off length of 0.15 mm shown in Figure 13 the variation becomes more significant with the film value varying between 0.12 and 1.2 μm with corresponding pressure variations between 0.5 and 3.5 GPa.

14
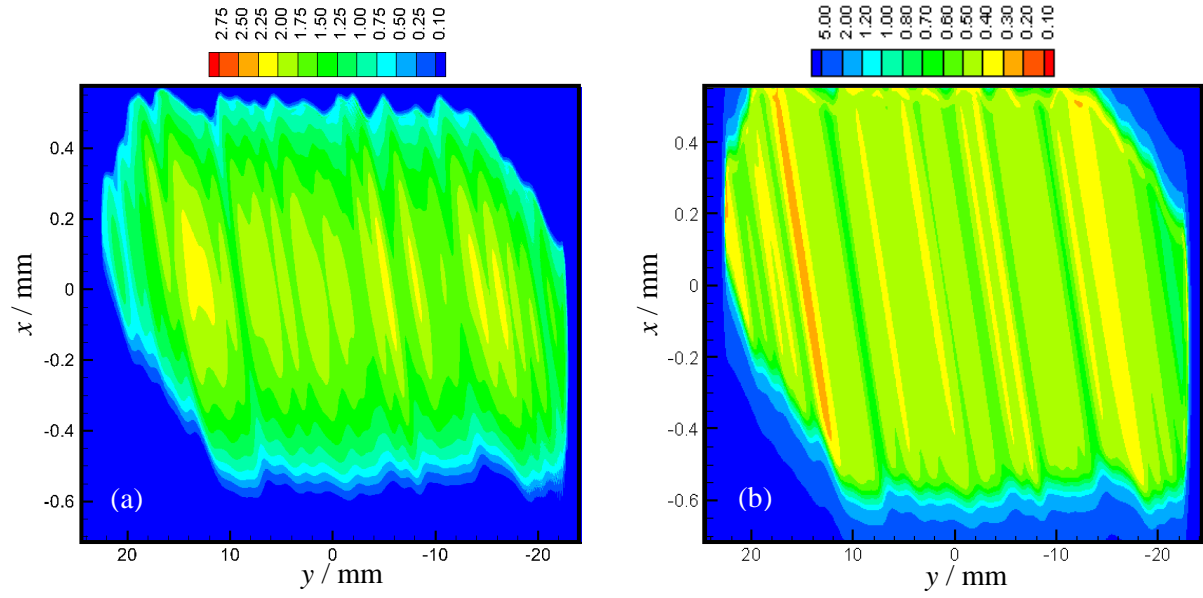
Figure 11. (a) Contours of (a) *p*/GPa and (b) *h*/μm for the EHL analysis at 80 °C
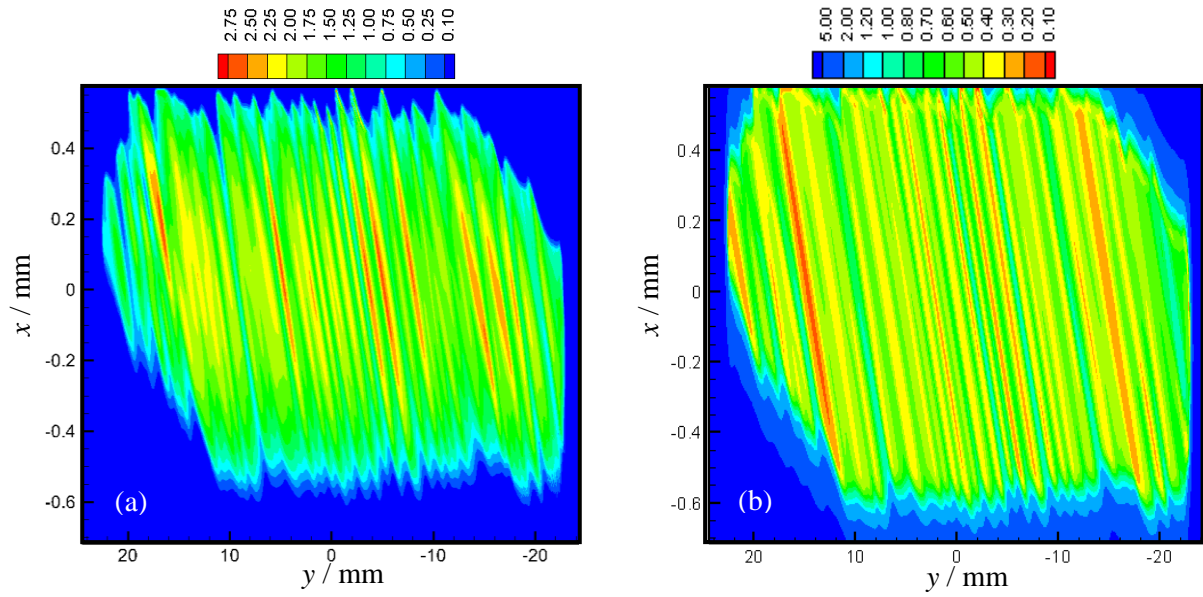with 0.5 mm cut-off profilometer profile errors.

Figure 12. Contours of (a) *p*/GPa and (b) *h*/μm for the EHL analysis at 80 °C
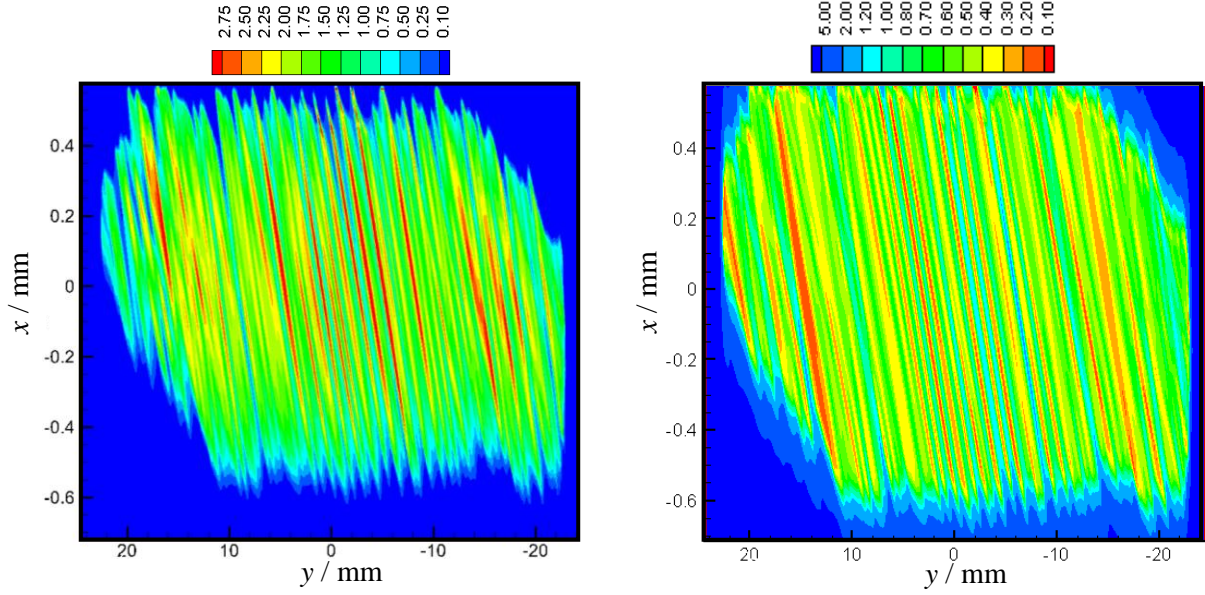with 0.25 mm cut-off profilometer profile errors.

15

Figure 13. Contours of (a) p/GPa and (b) h/μm for the EHL analysis at 80 °C
with 0.15 mm cut-off profilometer profile errors.

Figure 14 shows the pressure and film thickness variation for timestep 300 along the contact line for the profilometer profiles filtered with cut off lengths of 0.5 mm and 0.15 mm. This emphasises the sensitivity of the EHL results to the detailed geometry of the waviness features that are included in the involute error profiles. At the shorter cut off length more fine detail of the deviations from the ideal involute shape are brought through into the calculation and their effect is significant in causing the load not to be shared in anything like a uniform way along the contact line.
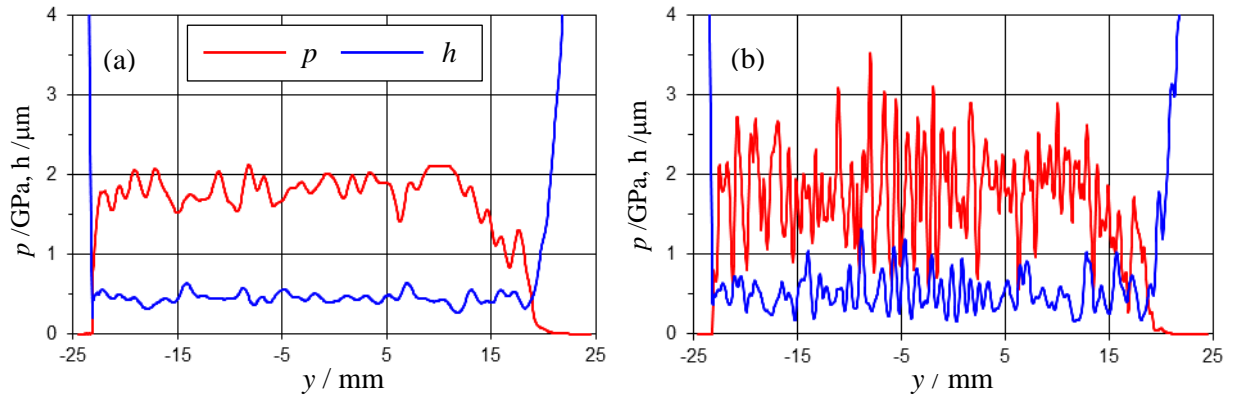

Figure 14. Sections of pressure and film thickness for $x = 0$,
(a) cut-off 0.5 mm, (b) cut-off 0.15 mm.

Figure 15 shows corresponding sections in the entrainment direction. At the 0.5 mm cut off setting the filter provides a waviness profile that has about two waves in the contact area and these have little effect on the pressure distribution which is not dissimilar to what would be seen for smooth surfaces.

16

However at the shorter cut off there are six waves in the contact area, the pressure response to these waves is significant but does not flatten them elastically.
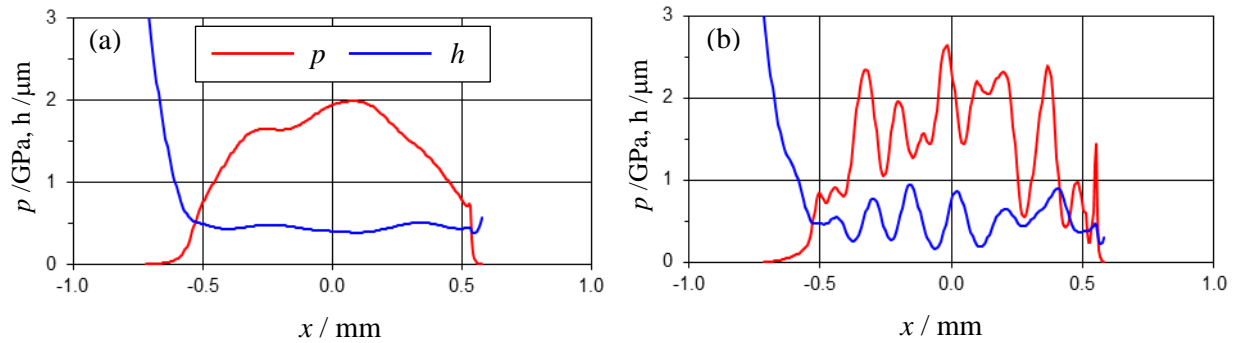

Figure 15. Sections of pressure and film thickness for $y = 0$,
(a) cut-off 0.5 mm, (b) cut-off 0.15 mm.

7. DISCUSSION AND CONCLUSIONS

The results presented in this paper quantifies the effects of measured profile deviations on the EHL lubricant film developed between helical gears. This gives a measure of the functional effect of profile deviations that are specified as part of a gear's quality rating. However quality numbers are principally associated with tolerances of the flank position and shape. The results presented in this contribution suggest that deviations in the profile may affect oil film formation to an extent that may not be appreciated, and that the way in which profile error measurement is carried out, and filtered, is an important factor that should be considered.

The error profiles used for these analyses are the as-manufactured profiles for test gears that are being run in endurance tests. The surface roughness has not been considered because it will be modified by plastic deformation of surface asperities during the tests. This is a process that takes place very rapidly converting the roughness to a series of rounded load bearing lands by plastic deformation [22, 23]. The effect of roughness measured at different stages in the endurance testing will be taken into account in future calculations, but it is informative to realise that profile waviness will interact with the roughness effects.

It can be concluded that:
- Local deviations of profile error curves that are within overall tolerances can cause significant differences in the way in which the EHL lubricant film carries the load.
- The filtering process that is involved in producing profile error curves is instrumental in determining lubricant pressure distributions and film thickness.

17

ACKNOWLEDGEMENTS

REFERENCES

[1] Kahraman, A. and Singh, R. Non-linear dynamics of a spur gear pair. *Journal of Sound and Vibration*. 142, 49-75, 1990.

[2] Fernandez, A., Iglesias, M., de-Juan, A., Garcia, P., Sancibrian, R. & Viadero, F. Gear transmission dynamic: Effects of tooth profile deviations and support flexibility. *Applied Acoustics,* 77, 138-149, 2014.

[3] Ottewill, J.R., Neild, S.A., Wilson, R.E. An investigation into the effect of tooth profile errors on gear rattle. *Journal of Sound and Vibration*, 329, 3495-3506, 2010.

[4] Ren, F. & Qin, D. Investigation of the effect of manufacturing errors on dynamic characteristics of herringbone planetary gear trains. *Proc. International Gear Conference 2014: Lyon*, 230-239, 2014.

[5] Li, S., Effects of machining errors, assembly errors and tooth modifications on loading capacity, load-sharing ratio and transmission error of a pair of spur gears. *Mechanism and Machine Theory,* 42(6), 698-726, 2007.

[6] Liu, X., Yang, Y., & Zhang, J. Investigation on coupling effects between surface wear and dynamics in a spur gear system. *Tribology International*, 101, 383-394, 2016.

[7] Li, S., Vaidyanathan, A., Harianto, J., and Kahraman, A. Influence of design parameters on mechanical power losses of helical gear pairs. Journal of Adv. Mechanical Design, Systems & Manufacturing, 3(2), 146-158, 2009.

[8] Simon, V. Thermo-EHL analysis of lubrication of helical gears. *Journal of Mechanisms, Transmissions, and Automation in Design*, 110, 330-338, 1988.

[9] Zhu, C., Liu, M., Liu, H., Xu, X., and Liu, L. A Thermal Finite Line Contact EHL Model of a Helical Pair. *Proceedings of the Institution of Mechanical Engineers - Part J: Journal of Engineering Tribology.* 227 (4) , 299–309, 2012.

[10] Barbieri, M., Lubrecht, A.A., Pellicano, F. Behaviour of lubricant fluid film in gears under dynamic conditions. *Tribology International*, 62, 37-48, 2013.

[11] Wang, Y. Q., He, Z. C., and Su, W., Effect of Impact Load on Transient Elastohydrodynamic Lubrication of Involute Spur Gears, *Tribology Transactions*, 55, 155–162, 2012

[12] Xue, J., Li, W., Qin, C. The scuffing load capacity of involute spur gear systems based on dynamic loads and transient thermal elastohydrodynamic lubrication. *Tribology International*, 79, 74-83, 2014.

[13] Evans, H.P., Snidle, R.W., Sharif, K.J., Shaw, B.A., Zhang, J. Analysis of micro-elastohydrodynamic lubrication and prediction of surface fatigue damage in micropitting tests on helical gears. *ASME Journal of Tribology*, 135(1), 011501-1, 2012.

[14] De la Cruz, M., Chong, W.W.F., Teodorescu, M., Theodossiades, S., Rahnejat, H. Transient mixed thermo-hydrodynamic lubrication in multi-speed transmissions. *Tribology International*, 49, 17-29, 2012.

[15] Brandao, J.A., Martins, R., Seabra, J.H.O., Castro, M.J.D. An approach to the simulation of concurrent gear micropitting and mild wear. *Wear*, 324-325, 64-73, 2015.

[16] Serest, A.E. & Akbarzadeh, S. Mixed-elastohydrodynamic analysis of helical gears using load-sharing concept. *Proceedings of the Institution of Mechanical Engineers - Part J: Journal of Engineering Tribology,* 228(3), 320-331, 2014.

[17] Liu, M., Zhu, C., Liu, H. A Micro-TEHL Finite Line Contact Model for a Helical Gear Pair. *Advances in Mechanical Engineering*, 7(1), 104790, 2014.

[18] Zhu, D., Ren, N., and Wang, Q. J. Pitting Life Prediction Based on a 3D Line Contact Mixed EHL Analysis and Subsurface von-Mises Stress Calculation. *ASME Journal of Tribology*, 131, 041501-1-8, 2009.

[19] Jamali, H. U., Sharif, K. J., Evans, H. P. and Snidle, R.W. The transient effects of profile modification on elastohydrodynamic oil films in helical gears. *Tribology Transactions* , 58:1, 119-130, 2014.

[20] Evans, H. P, and Hughes, T. G. Evaluation of deflection in semi-infinite bodies by a differential method. *Proc Instn Mech Engrs*, Part C: Journal of Mechanical Engineering Science, (214)568-583, 2000.

[21] Jamali, H. U., Analysis of helical gear performance under elastohydrodynamic lubrication, PhD thesis, Cardiff University, 2015

[22] Clarke A., Weeks I., Evans H.P., Snidle R.W., An investigation into mixed lubrication conditions using electrical contact resistance techniques. *Tribology International*, 93B, 709-716, 2014

[23] Clarke A., Weeks I., Snidle R.W., Evans HP, Running-in and micropitting behaviour of steel surfaces under mixed lubrication conditions. *Tribology International*, 2016, 10.1016/j.triboint.2016.03.007